Periodico di Mineralogia (2011), 80, 2, 247-266 DOI: 10.2451/2011PM0019

PERIODICO di MINERALOGIA
established in 1930

An International Journal of
MINERALOGY, CRYSTALLOGRAPHY, GEOCHEMISTRY, ORE DEPOSITS, PETROLOGY, VOLCANOLOGY
and applied topics on *Environment*, *Archeometry* and *Cultural Heritage*

Vein mineral assemblage in partially serpentinized peridotite xenoliths from Hyblean Plateau (south-eastern Sicily, Italy)

Fabio C. Manuella

Dipartimento di Scienze Geologiche, Università di Catania, C.so Italia 57, I-95129 Catania - Italy
fmanuella@alice.it

Abstract

A mineralogical study was performed on seven selected peridotite xenoliths, found in diatremic tuff-breccia deposits from Valle Guffari (Hyblean Plateau, Sicily, Italy), in order to investigate evidence for serpentinization. Petrographic examinations of spinel-harzburgites revealed the presence of the pervasive network of composite serpentine veins, suggesting a variable degree of alteration of 50-80%.

Veins were characterized by X-ray Powder Diffraction (XRPD), which allowed the identification of chrysotile $2M_{c1}$ and lizardite $1T$. No peaks referable to antigorite polymorphs were detected. Microprobe WDS (wavelength dispersion system) data evidenced a different iron content between chrysotile [average composition $(Mg_{2.58}Fe^{2+}_{0.27}Al_{0.01})_{\Sigma 2.86}Si_{2.06}O_5(OH)_4$, Fe/(Fe+Mg) = 0.09] and lizardite [average composition $(Mg_{2.49}Fe^{2+}_{0.37}Al_{0.01})_{\Sigma 2.87}Si_{2.05}O_5(OH)_4$, Fe/(Fe+Mg) = 0.12]. Chlorine was detected in both polytypes, with an average concentration of 0.09 wt% in chrysotile and 0.05 wt% in lizardite.

A series of cogenetic secondary minerals are enclosed in serpentine veins, described hereunder:

a) Sulphides, predominantly S-poor phases (atomic sulphur/metal ratio < 1), which are heazlewoodite [average composition $(Ni_{2.75}Fe_{0.09})_{\Sigma 2.84}S_2$] and godlevskite [mean composition $(Ni_{8.52}Fe_{0.63})_{\Sigma 9.15}S_8$), and to a lesser extent by S-rich sulphides (S/M > 1), such as millerite [mean composition $(Ni_{0.95}Fe_{0.03})_{\Sigma 0.98}S$] and polydymite-violarite solid solution [mean composition $(Fe_{1.38}Ni_{1.69})_{\Sigma 3.07}S_4$].

b) Interstitial dendritic aggregates of Na-rich sylvite, whose molar ratio of NaCl/(NaCl+KCl) (X_{NaCl}) varies from 0.03 to 0.21.

c) Widespread veinlets of (Ca, Na, S)-rich phosphates (CaO 50.30-52.70 wt%, Na_2O 1.50-3.10 wt%, P_2O_5 31.76-34.60 wt%, SO_3 7.40-12.60 wt%), whose chemical composition is similar to (Na, S)-rich apatite-(CaOH)-M (CaO 48.70-54.30 wt%, Na_2O 0.10-3.90 wt%, P_2O_5 32.01-40.82 wt%, SO_3 0.40-11.40 wt%).

d) Aragonite veins.

e) Fe-rich saponite (FeO 5.20-13.50 wt%).

f) Chalcedony.

The studied secondary mineral assemblage hints that serpentinization reactions were triggered in the ultramafic core-complex, forming the Hyblean basement, by hypersaline aqueous solutions, most likely deriving from seawater, in a temperature range from 250 °C to 350-400 °C at a pressure below 0.2 GPa.

Partially serpentinized harzburgite xenoliths can be distinguished on the basis of secondary mineral assemblages. Most of the studied xenoliths contain abundant S-poor sulphides, which are indicative of reducing conditions (f_{O_2} from -40 to -32) and high temperature (~ 400 °C; Fleet, 1988), likely referable to the early stage of serpentinization. Only two xenoliths include S-rich sulphides, aragonite, saponite, and chalcedony, which are the products of the incipient carbonation and saponitization of serpentine, suggesting a relatively oxidant environment (f_{O_2} from -34 to -30) and low to moderate temperature (below 300 °C).

The dominance of xenoliths bearing S-poor sulphides, and the occurrence of NaCl-KCl solid solutions, whose values of X_{NaCl} support a temperature range of 200-380 °C, would suggest that serpentine veins and their related secondary minerals were produced before the diatreme eruption (Tortonian, Carlentini Formation). In fact, a post-depositional alteration would imply strongly oxidizing conditions (above the Hematite-magnetite buffer) and low temperature, certainly incompatible with the formation of the observed secondary minerals. The timing of serpentinization, in the Hyblean lower crust, can be deduced from the age of hydrothermal zircons, found in a blackwall-type metasomatite xenolith, which was previously dated back to Early Triassic, by U-Pb analyses.

Key words: serpentinization; hydrothermal system; sulphides; Hyblean Plateau; xenoliths.

Introduction

The hydration of olivine and pyroxene in ultramafic rocks triggers a set of chemical reactions, known as serpentinization, whose rate is faster in the temperature range of 250-300 °C (Bach et al., 2004, and references therein). This process is accompanied by several modifications in the serpentinized rocks, such as volume increase (about 40-60% for contemporaneous alteration of olivine and orthopyroxene; Hostetler et al., 1966; MacDonald and Fyfe, 1985), geophysical effects (magnetic and seismic anomalies; Horen et al., 1996; Schroeder et al., 2002), and even local geochemical variations (Bach and Früh-Green, 2010) which control solid solutions and metastable reactions.

Moreover, the exothermic hydration reactions produce a more or less intense heat-flow (290 KJ/Kg consumed forsterite; MacDonald and Fyfe, 1985) which promotes the formation and maintenance of hydrothermal systems (Emmanuel and Berkowitz, 2006). Accordingly, recent oceanographic cruises discovered numerous serpentinite-hosted hydrothermal fields (HF) in slow- and ultra-slow spreading ridges, particularly in Mid-Atlantic Ridge (MAR): i.e., Saldanha (36°34′N; Dias and Barriga, 2006), Rainbow (36°14′N; e.g., Pikovskii et al., 2004), Lost City (30°N; e.g., Boschi et al., 2006), Logatchev (14°45′N; Schmidt et al., 2007), Nibelungen (8°S; Koschinsky et al., 2008).

Serpentinization can be influenced by several factors (Bach and Früh-Green, 2010), such as pressure, temperature, water/rock ratio, and redox conditions, which regulate the formation of secondary mineral assemblages.

On this ground, the present study is aimed at investigating serpentine polytypes and other

secondary minerals, in some partially serpentinized peridotite xenoliths, in order to infer the physico-chemical conditions during serpentinization.

Geological background

The Hyblean Plateau (south-eastern Sicily, Italy) is traditionally considered an uplifted emerged portion of the Pelagian foreland, belonging to the African continental crust (Lentini et al., 1996; Catalano et al., 2000), although structural and geophysical features of the plateau differ from those of the African foreland (Brancato et al., 2009). In this regard, the only direct evidence for the nature of the Hyblean lithospheric basement comes from deep-seated xenoliths from some diatremic tuff-breccia deposits of Upper Miocenic age (Scribano, 1986). The dominant lithologies are represented by spinel-lherzolites and harzburgites (Scribano, 1987), exhibiting chemical composition and isotopic signatures consistent with a depleted mantle origin, minor sheared oxide-gabbros (Scribano et al., 2006a), along with various sedimentary and volcanic rocks which belong to the Meso-Cenozoic succession.

Surprisingly, no rocks typical of continental crust (e.g., granites, felsic metaigneous and metasedimentary lithologies; Sapienza and Scribano, 2000) have been ever found. This evidence agree with the lack of contamination by continental crust rocks in the Hyblean lavas (Trua et al., 1998; Bianchini et al., 1999), based on Sr-Nd-Pb isotopic data, which excluded two hypotheses proposed by Sapienza and Scribano (2000), which are (1) complex tectonic modification of a previous thinned continental crust, or (2) sever erosion of continental crust during a hypothetical exhumantion. Petrographic and geochemical comparison of oxide-rich gabbro xenoliths with gabbros collected in fracture zones of slow-spreading ridges, induced Scribano et al. (2006a) to infer that the Hyblean lower crust is formed from an oceanic core-complex, tectonically exposed at the sea-floor of an early oceanic domain, probably the Permo-Thetys Ocean (Vai, 2003). Moreover, Punturo et al. (2000) asserted that (1) Th/Ta ratios (< 1), in some peridotite and feldspar-bearing xenoliths, are below the values of the same ratio in the lower continental crust, and (2) La/Nb ratios (< 1.4), in some crustal xenoliths, match values measured in oceanic plateaux.

Additionally, Scribano et al. (2006b) inferred the existence of a fossil abyssal-type hydrothermal system in the Hyblean basement, according to petrological and mineralogical investigations on a set of hydrothermally altered gabbroic xenoliths. Among the numerous hydrothermal minerals, albite, aegirine-augite, titanite, sulphides, and even hydrothermal zircons are worth of notice, in addition to traces of abiogenic aliphatic-aromatic hydrocarbons (Ciliberto et al., 2009).

Methods and Techniques

All samples were studied in thin polished sections by means of a polarizing ZEISS microscope, in order to evaluate microtexture of serpentine minerals and their related secondary phases.

Whole-rock geochemical analyses were obtained by Punturo (1999) at the Dipartimento di Scienze Geologiche di Catania (Italy) by means of X-ray fluorescence (XRF) with a Philips PW2404 WD-XRF on powder pellets; XRF data were integrated with loss on ignition (L.O.I.) and Fe^{2+}/Fe^{3+} determination by $KMnO_4$ titration.

Detailed observations were performed at the Dipartimento di Scienze Geologiche, Università di Catania (Italy), using a TESCAN-VEGA\\LMU scanning electron microscope (SEM) equipped with an EDAX Neptune XM4-60 microanalysis tool working in energy

dispersive spectrometry (EDS), operating in backscattered electron mode at accelerating voltage 20 kV and beam current 0.2 nA.

Quantitative analyses of serpentine and sulphides were obtained at the Dipartimento di Scienze della Terra, Università di Milano (Italy), using a JEOL Superprobe 8200 equipped with 5 WDS (wavelength dispersion system) spectrometers, using an accelerating voltage of 15 kV and a beam current of 15 nA.

Crystalline phases were identified also by X-ray powder diffractometer Siemens D5000, equipped with Cu anode (K_α = 1.5406 Å), filter Ni, ΔV = 40 kV, I = 30 mA, windows of 2 mm, 1 mm, 0.2 mm. Measurements were carried out as a continuous scan from 3° to 100° 2θ, with a calculated step size of 0.020° 2θ, and a calculated time per step of 1.00 s.

Studied materials

In the present work, seven partially serpentinized peridotite xenoliths (50-80% degree of serpentinization), represented by spinel-harzburgites, were considered in order to characterise serpentine veins and other secondary minerals enclosed. Petrographic observations (Punturo, 1999; Punturo et al., 2000) recognized a protogranular texture formed from olivine (60-77 %), orthopyroxene (13-27 %), clinopyroxene (Cr-diopside; 3-12 %), and Cr-Al spinel (3-5 %). These xenoliths come from the diatremic tuff-breccia deposits of Valle Guffari (south-western side of Mt. Lauro, Hyblean Plateau; Figure 1), which represents the most important xenolith occurrence in the Hyblean Plateau.Whole-rock geochemical analyses (Table 1) and representative microprobe WDS data (Table 2) of primary minerals (Punturo, 1999) constituting peridotite are reported.

The average Mg# values of the peridotite olivine is 0.91. The Cr/(Cr + Al) ratio (Cr#) from 0.23 to 0.29 and Mg# from 0.7 to 0.8 of spinels agrees with values of abyssal peridotites reported

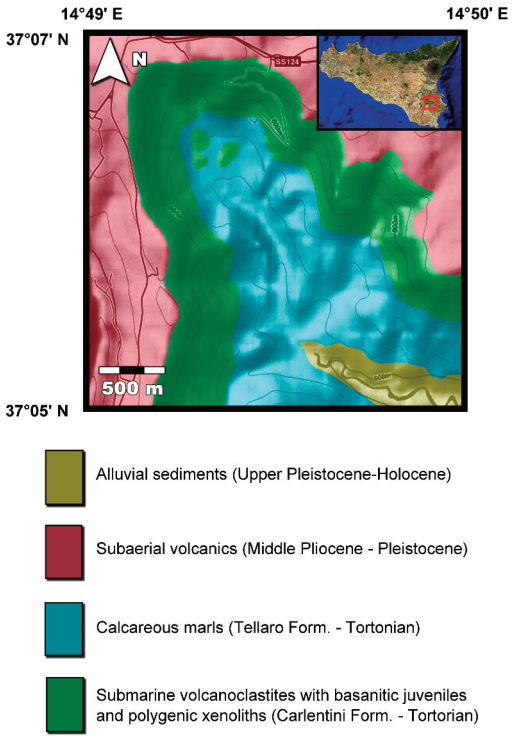

Figure 1. Geological sketch of Valle Guffari (south-eastern Sicily, Italy), after Beccaluva et al. (1991).

by Le Mée et al. (2004). The Mg# values of orthopyroxene vary from 0.90 to 0.91 with CaO > 1 wt%. Minor Cr-diopside exhibits a narrow range of compositional variations ($En_{54}Wo_{44}Fs_2$ - $En_{52}Wo_{44}Fs_4$). The major-element composition in the peridotites also suggests a moderate to high degree of depletion (whole rock Al_2O_3 < 2 wt%, TiO_2 < 0.2 wt%).

Results

Serpentine polytypes

Petrographic study of peridotite xenoliths revealed the pervasive occurrence of composite picrolite veins (Riordon, 1955; Figure 2A, B), constituted by chrysotile $2M_{c1}$ and lizardite $1T$, which were analysed by both X-ray powder

Table 1. Whole rock analyses and trace elements of seven harzburgite xenoliths (Punturo, 1999).

wt%	P 1	P 2	P 3	P 4	P 5	P 6	P 7
SiO_2	40.55	39.51	40.18	43.18	43.11	39.32	42.77
TiO_2	0.05	0.04	0.18	0.04	0.03	0.04	0.13
Al_2O_3	1.31	1.19	1.25	1.01	0.72	0.74	1.29
Fe_2O_3	4.34	8.17	9.43	4.71	7.04	4.79	7.20
FeO	4.27	1.55	0.67	4.90	3.16	3.75	3.52
MnO	0.11	0.11	0.12	0.13	0.13	0.12	0.14
MgO	37.76	36.41	34.81	38.37	33.84	38.65	37.34
CaO	3.75	4.77	4.57	3.20	4.20	4.78	2.30
Na_2O	0.11	0.11	0.15	0.06	0.07	0.07	0.09
K_2O	0.03	0.04	0.02	0.03	0.05	0.01	0.03
P_2O_5	0.17	0.20	0.07	0.11	0.15	0.15	0.10
L.O.I.	7.56	7.91	8.57	4.26	7.49	7.57	5.09
Tot.	100.01	100.01	100.02	100.00	99.99	99.99	100.00
La	0.00	1.80	1.30	0.20	1.30	0.00	0.00
Ce	0.82	0.00	0.00	0.00	8.12	0.00	0.00
V	79	70	82	44	54	63	51
Cr	2979	2839	3145	2656	2440	3116	2431
Co	119	126	112	121	130	116	124
Ni	2327	2427	2111	2533	2714	2319	2567
Zn	50.0	55.4	63.7	50.9	56.6	49.6	63.3
Sr	201	332	130	160	238	261	119
Rb	0.95	1.87	0.26	2.04	1.30	0.00	0.00
Ba	24	17	24	25	17	15	24
Th	2.89	2.80	5.37	5.88	4.04	1.77	0.00
Nb	0.00	0.00	0.00	0.00	0.00	0.00	0.00
Pb	3.90	2.00	5.00	3.00	0.00	2.00	6.00
Zr	2.80	5.90	24.60	2.60	2.70	0.70	11.10
Y	0.00	2.20	4.20	2.10	1.70	2.30	0.00

diffraction (XRPD; Figure 3) on hand-picked veins, and microprobe WDS (Table 3) on thin polished sections. The latter analyses showed that serpentine polytypes contain moderate amounts of chlorine (0.08 - 0.09 wt% and 0.04 - 0.05 wt%, respectively).

Structural recalculations of serpentine polytypes, based on 7 (O, Cl), exhibit compositional ranges (in apfu) for lizardite which are 2.36-2.61 (Mg), 0.25-0.45 ($Fe_{tot.}$), 0.003-0.015 ($Al^{[VI]}$) and 1.95-2.12 (Si), instead for chrysotile are 2.44-2.79 (Mg), 0.12-0.39 ($Fe_{tot.}$), 0.002-0.013 ($Al^{[VI]}$) and 2.04-2.14 (Si).

Differences between the two serpentine minerals can be highlighted considering the compositional patterns of aluminium and iron (Figure 4), as suggested by Viti and Mellini (1997), because these two elements represent the main substitutions for magnesium in octahedral sheets. Lizardite is enriched in iron and aluminium, compared to the amounts of the same elements in chrysotile, regardless of Si ions which saturate tetrahedral site.

Table 2. Representative microprobe WDS analyses of four primary minerals of peridotite (Punturo, 1999), with relative calculated standard deviations (S.D.).

wt%	Ol	*S.D.*	Sp	*S.D.*	Opx	*S.D.*	Cpx	*S.D.*
SiO_2	41.18	0.31	0.14	0.03	55.10	0.21	51.97	0.29
TiO_2	0.00	0.00	0.51	0.05	0.20	0.04	0.56	0.16
Al_2O_3	0.00	0.00	43.16	2.33	4.51	0.33	5.47	0.67
Cr_2O_3	0.00	0.00	22.13	2.22	0.66	0.14	1.22	0.24
FeO	9.9	0.42	14.03	0.96	6.24	0.18	3.59	0.15
MnO	0.12	0.03	0.13	0.05	0.14	0.05	0.09	0.06
MgO	49.96	0.27	19.24	0.51	33.01	0.14	17.03	0.25
CaO	0.13	0.03	0.00	0.00	1.23	0.15	19.71	0.64
Na_2O	0.00	0.00	0.00	0.00	0.11	0.02	1.13	0.24
Total	101.29		99.33		101.19		100.75	

Ol = olivine; Sp = spinel; Opx = orthopyroxene; Cpx = clinopyroxene.

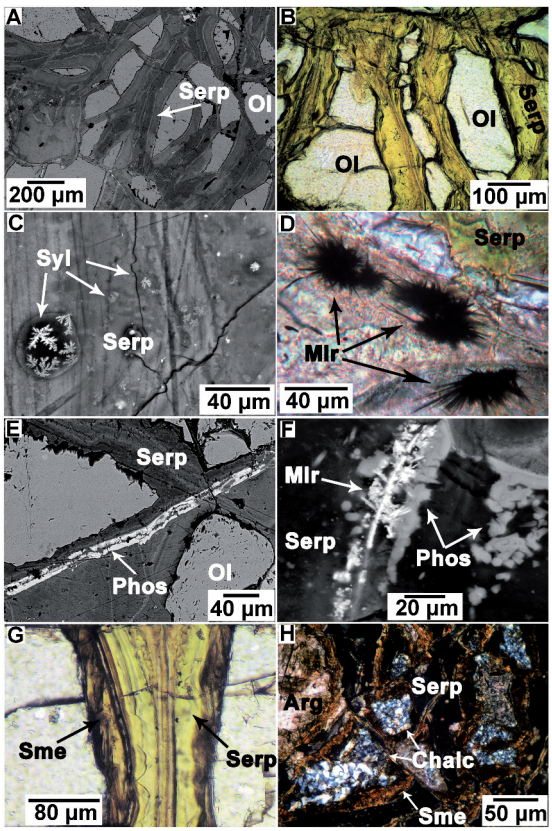

Figure 2. A and B Composite picrolite veins with relicts of olivine grains (Ol). C Dendritic hoppers of Na-rich sylvite (Syl) in serpentine. D Acicular aggregates of millerite (Mlr) in serpentine (Serp). E and F Veinlets and crystals of phosphate (Phos) in serpentine. G Incipient saponitization of serpentine. H Chalcedony (Chalc) surrounded by a clayey rim (Sme) with mesh serpentine and aragonite (Arg).

Other secondary minerals

Detailed back-scattering SEM observations proved the presence of interstitial dendritic hoppers of Na-rich sylvite inside serpentine veins (Figure 2C), whose molar ratio NaCl/(NaCl+KCl) (X_{NaCl}) ranges from 0.03 to 0.21 (Table 4).

The secondary sulphide assemblage (Table 5; Figure 5) in serpentine consists of heazlewoodite (Ni_3S_2), godlevskite (Ni_9S_8), millerite (NiS; Figure 2D), and polydymite-violarite solid solution (polydymite-ss; Misra and Fleet, 1974).

Microprobe analyses of S-poor sulphides, with atomic sulphur/metal ratio (*S/M*) < 1 (Frost and Beard, 2007; Klein and Bach,

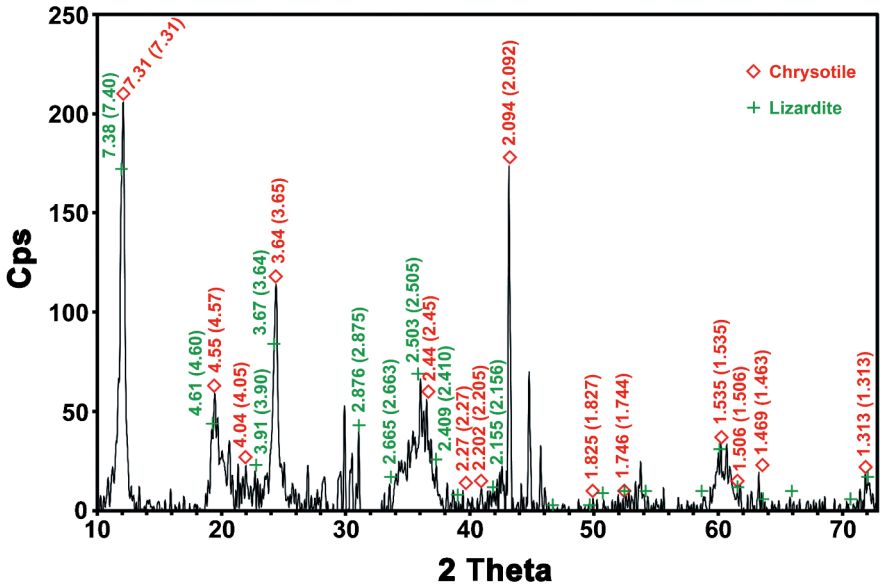

Figure 3. X-ray powder diffraction pattern of hand-picked veins of chrysotile and lizardite, with the observed Bragg reflections in Å, and standard values (in brackets) relative to JCPDS cards no. 31-808 and 18-779, respectively.

2009), revealed that heazlewoodite (mean composition $Ni_{2.75}Fe_{0.09}S_2$) has an iron content variable between 0.08 and 0.10 mol%, and a *S/M* ratio of 0.70. Godlevskite (mean composition $Ni_{8.52}Fe_{0.63}S_8$) exhibits a variable enrichment in Fe (up to 1.21 mol%), and a *S/M* ratio which varies from 0.88 to 0.92. Differently, compositional data of S-rich sulphides, with atomic *S/M* ratio > 1, showed that millerite (mean composition $Ni_{0.95}Fe_{0.03}S$) has an iron content of 0.03 mol%, and a *S/M* ratio varying from 1.00 to 1.04. Polydymite-solid solution (mean composition $Fe_{1.38}Ni_{1.69}S_4$) is enriched in iron (1.38 mol%), copper (0.05 mol%) and lead (0.02 mol%); it has an atomic *S/M* ratio of 1.27. Some of these sulphide minerals were also detected by X-ray powder diffraction analyses, such as godlevskite (JCPDS card no. 22-1193: 2.85, 1.80, 1.66, 3.26, 2.10, 2.33 Å), heazlewoodite (JCPDS card no. 30-863: 2.88, 4.09, 1.66, 1.83, 2.38 Å), and millerite (JCPDS card no. 12-41: 2.78, 1.86, 2.51, 4.81, 2.23 Å).

Widespread phosphate veinlets (Figure 2E, F), pervading serpentine veins, exhibit a chemical affinity (Table 6) with apatites reported by Shiga and Urashima (1987) and Chakhmouradian and Medici (2006).

Some xenoliths contain commonly carbonate veins, identified as aragonite by its main reflections in XRPD (JCPDS card 41-1475: d_{111} = 3.40 Å, d_{021} = 3.27 Å, d_{200} = 2.48 Å, d_{130} = 2.34 Å). X-ray diffraction analyses of clayey plugs near serpentine veins (Figure 2G), observed in two carbonated xenoliths (Figure 2G), show a basal reflection (d_{001}) at 15.45 Å, and weak peaks at 3.08, 5.14, 7.77 and 3.78 attributed to (005), (003), (002) and (004) Bragg reflections (JCPDS card no. 29-1491). These lines agree with data reported by Parthasarathy et al. (2003), along with *d* (060) reflection at 1.535 Å, which confirm this clay mineral is a trioctahedral smectite, particularly iron-rich

Table 3. Electron microprobe WDS analyses of serpentine polytypes and saponite, with relative structural recalculations, based on 7 and 22 anhydrous oxygens, respectively.

wt%	Chrysotile				Lizardite				Saponite		
Samples	P3	P2	P4	P1	P2	P3	P2	P2	P5	P5	P5
SiO_2	43.39	42.08	43.39	41.46	36.49	42.03	42.78	42.76	55.21	51.02	51.20
Al_2O_3	0.12	0.23	0.03	0.03	0.13	4.46	0.05	0.27	0.09	0.13	0.32
TiO_2	0.01	0.00	0.00	0.01	0.00	0.05	0.00	0.00	0.00	0.01	0.05
Cr_2O_3	0.04	0.00	0.00	0.00	0.05	0.14	0.00	0.03	0.03	0.05	0.13
$FeO_{tot.}$	9.92	6.55	6.00	2.81	10.10	9.39	8.28	6.30	13.56	12.82	5.23
MnO	0.13	0.09	0.11	0.13	0.15	0.09	0.07	0.07	0.05	0.04	0.03
MgO	35.60	36.46	33.19	38.03	32.63	30.31	34.72	36.49	18.81	17.53	22.05
CaO	0.07	0.06	0.34	0.06	0.05	0.08	0.06	0.07	0.71	0.51	0.45
Na_2O	0.02	0.01	0.04	0.02	0.02	0.02	0.01	0.02	0.12	0.06	0.05
K_2O	0.01	0.00	0.03	0.01	0.01	0.04	0.00	0.01	0.72	0.76	0.28
NiO	0.32	0.07	0.11	0.07	0.26	0.17	0.24	0.05	0.67	0.48	0.36
Cl	0.09	0.08	0.09	0.08	0.05	0.05	0.04	0.04	0.00	0.00	0.00
Total	89.73	85.63	83.34	82.71	79.95	86.83	86.25	86.13	89.99	86.40	80.15
apfu											
Si	2.039	2.036	2.139	2.039	1.953	2.021	2.070	2.051	7.995	7.978	7.963
Al^{VI}	0.007	0.013	0.002	0.002	0.008	0.253	0.003	0.015	0.015	0.023	0.058
Ti	0.000	0.000	0.000	0.000	0.000	0.002	0.000	0.000	0.000	0.001	0.005
Cr	0.002	0.000	0.000	0.000	0.002	0.005	0.000	0.001	0.003	0.006	0.016
Fe^{2+}	0.390	0.265	0.247	0.116	0.452	0.377	0.335	0.253	1.642	1.676	0.680
Mn	0.005	0.004	0.005	0.005	0.007	0.004	0.003	0.003	0.007	0.005	0.004
Mg	2.494	2.630	2.439	2.788	2.603	2.172	2.504	2.609	4.061	4.087	5.112
Ca	0.003	0.003	0.018	0.003	0.003	0.004	0.003	0.004	0.111	0.085	0.076
Na	0.002	0.001	0.004	0.002	0.002	0.002	0.001	0.001	0.033	0.019	0.015
K	0.001	0.000	0.002	0.001	0.001	0.003	0.000	0.001	0.134	0.151	0.055
Ni	0.012	0.003	0.004	0.003	0.011	0.007	0.009	0.002	0.078	0.064	0.045
Cl	0.014	0.013	0.015	0.013	0.009	0.008	0.007	0.007	0.000	0.000	0.000
Tot. Cations	4.955	4.955	4.860	4.959	4.537	4.850	4.928	4.940	14.079	14.095	14.029
X_{Fe}	0.14	0.09	0.09	0.04	0.15	0.15	0.12	0.09	0.29	0.29	0.12

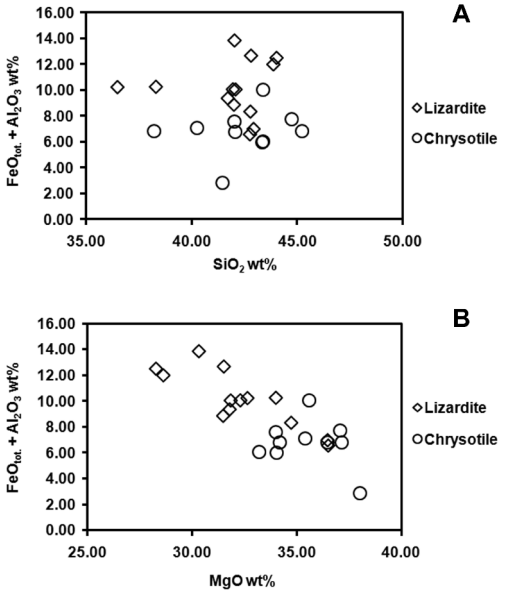

Figure 4. Chemical comparison of chrysotile and lizardite in serpentine veins.

saponite. Microprobe WDS analyses (Table 3) show that saponite contains considerable amounts of iron, ranging from 0.68 to 1.68 apfu. In addition, chalcedony was found in one of the carbonated xenoliths (Figure 2H).

Discussion

Conditions of serpentinization and formation of secondary minerals

The examined Hyblean peridotite xenoliths bear evidence for serpentinization represented by composite serpentine veins, whose formation is generally attributed to a crack-seal mechanism (Riordon, 1955; Andreani et al., 2004). This process is triggered by the opening of cracks which enhanced the pore fluid circulation (MacDonald and Fyfe, 1985), promoting the hydrolysis of olivine and pyroxene, in the thermal ranges of 151-328 °C and 195-438 °C respectively (Silantyev et al., 2009). The formation of chrysotile and lizardite occurs at temperature up to 350-400 °C (Bach et al., 2004) according to reaction 1 (Schroeder et al., 2002).

(1) $(Mg, Fe)_2SiO_{4(s)} + (Mg, Fe)SiO_{3(s)} + 2H_2O_{(liq)} \rightarrow (Mg, Fe)_3Si_2O_5(OH)_{4(s)}$
$\Delta H°_f = -16$ Kcal·mol^{-1} (MacDonald and Fyfe, 1985)

The studied serpentine polytypes exhibit a remarkable iron content (6-10 wt% FeO) as evidenced by high X_{Fe} (Fe/Fe+Mg) in chrysotile (0.04-0.14) and lizardite (0.09-0.15). Field observations on abyssal peridotites (Oufi et al., 2002) demonstrated that iron fractionation in

Table 4. EDS micro-analyses of Na-rich sylvite.

Samples wt%	P 4	P 4	P 4	P 1	P 6	P 6	P 4
Na	1.09	1.39	2.29	2.41	3.31	4.40	6.79
K	51.31	50.54	50.07	49.48	48.22	47.24	43.99
Cl	47.60	48.08	47.64	48.11	48.47	48.37	49.22
Tot.	100.00	100.00	100.00	100.00	100.00	100.00	100.00
moles							
NaCl	0.05	0.06	0.10	0.10	0.14	0.19	0.30
KCl	1.31	1.29	1.28	1.27	1.23	1.21	1.13
X_{NaCl}	0.03	0.04	0.07	0.08	0.10	0.14	0.21

Table 5. WDS micro-analyses of Ni sulphides, with relative atomic sulphur/metal ratios (S/M).

wt%	Heazlewoodite			Godlevskite					Millerite		Polydymite-ss
Samples	P2	P1	P3	P1	P2	P2	P2	P2	P4	P5	P5
Fe	2.19	2.00	2.48	0.00	0.00	1.75	3.26	8.61	1.71	1.95	24.72
Ni	70.17	69.95	69.88	67.50	66.87	65.27	62.66	58.60	62.45	61.65	31.78
Cu	0.00	0.00	0.00	0.00	0.00	0.00	0.00	0.00	0.00	0.00	1.11
Pb	0.00	0.00	0.00	0.00	0.00	0.00	0.00	0.00	0.00	0.00	1.27
S	27.64	28.05	27.64	32.50	33.13	32.98	33.14	32.79	35.32	36.41	41.12
Tot.	100.00	100.00	100.00	100.00	100.00	100.00	100.00	100.00	100.00	100.00	100.00
apfu											
Fe	0.09	0.08	0.10	0.00	0.00	0.24	0.45	1.21	0.03	0.03	1.38
Ni	2.77	2.72	2.76	9.08	8.82	8.65	8.26	7.81	0.97	0.93	1.69
Cu	0.00	0.00	0.00	0.00	0.00	0.00	0.00	0.00	0.00	0.00	0.05
Pb	0.00	0.00	0.00	0.00	0.00	0.00	0.00	0.00	0.00	0.00	0.02
S	2.00	2.00	2.00	8.00	8.00	8.00	8.00	8.00	1.00	1.00	4.00
S/M	0.70	0.71	0.70	0.88	0.91	0.90	0.92	0.89	1.00	1.04	1.27

serpentine depends on the degree of serpentinization (D.S.). In fact, iron tends to be partitioned into serpentine (FeO > 5 wt%) in partially serpentinized peridotites (D.S. < 75%), and its concentration progressively decreases to < 3.5 wt% in highly serpentinized rocks (D.S. > 75%). The upper limit of FeO amount in serpentine can vary from 16 wt% in lizardite to 9 wt% in chrysotile (Korytkova et al., 2007, and references therein).

WDS-microprobe analyses of chrysotile and lizardite detected moderate amounts of chlorine (0.04-0.09 wt% Cl), which are compatible with values recorded in oceanic serpentines ranging from 0.03 to 0.50 wt% (e.g., Sharp and Barnes, 2004; Miura et al., 1981), certainly attributed to seawater-peridotite interaction. In fact, chlorine can enter serpentine structure as substitution both of inner and outer hydroxyl groups, in tetrahedral and octahedral sheets (Anselmi et al., 2000).

Interstitial Na-rich sylvite aggregates were observed in serpentine veins by SEM investigations, as previously noticed in oceanic serpentinites by Sharp and Barnes (2004). Chemical analyses showed these grains are constituted by NaCl-KCl solid solutions, similarly to data reported by Scambelluri et al. (1997), which probably crystallised in the thermal range of 200-380 °C (Figure 6; Waldbaum, 1969) in agreement with their molar fraction X_{NaCl} (0.03-0.21).

The formation of chlorides in serpentine was explained by Sharp and Barnes (2004) according to reaction (1), in which pure water is replaced by seawater (reaction 2). The hydration of olivine and consequent incorporation of OH groups in serpentine consumed water, leading to residual hypersaline solutions and finally to precipitation of chlorides.

(2) $(Mg, Fe)_2SiO_{4(s)} + (Mg, Fe)SiO_{3(s)} + 2H_2O_{(liq)} + (Na^+, K^+)_{(aq)} + Cl^-_{(aq)} \rightarrow (Mg, Fe)_3 Si_2O_5 (OH)_{4(s)} + (Na, K)Cl_{(s)}$

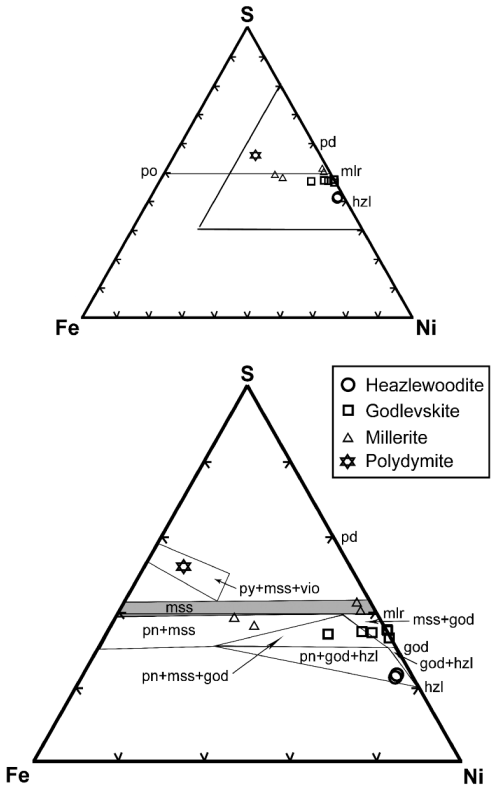

Figure 5. Fe-Ni-S ternary plots reporting chemical compositions, on the basis of atomic proportions of sulphides (see Table 5). Delimited areas represent stability fields of sulphide assemblages as reported by Ueno et al. (2000), in their diagram Fe-Ni-S at 400 °C determined by dry synthesis. The grey shaded area is the stability field of monosulphide solid solution. Mineral abbreviations: Po, pyrrhotite; Mlr, millerite; Pd, polydymite; Hzl, heazlewoodite; Vio, violarite; Mss, monosulphide solid solution; Pn, pentlandite.

This process can be favoured by restricted diffusion of salt ions through serpentine, because it behaves as a semipermeable membrane similarly to clays, in consequence of its low permeability (10^{-11} to 10^{-12} darcies; MacDonald and Fyfe, 1985).

Field and laboratory experiences (e.g., Southgate, 1982; Saito et al., 1987) demonstrated that dendritic habit of aggregates is produced by rapid precipitation from supersaturated aqueous solutions.

Among secondary minerals hosted in serpentine veins, secondary sulphide assemblage provides useful constraints on f_{O_2} and f_S (Delacour et al., 2008). The stability of these minerals is governed by reaction: $2S_2 + 2H_2O \leftrightarrow 2H_2S + O_2$ (Klein and Bach, 2009), which highlights the fact that significant variations of

Table 6. EDS micro-analyses of (Ca, Na, S)-rich phosphate veinlets.

	(Ca, Na, S)-rich phosphate veinlets				Shiga and Urashima (1987)		Chakhmouradian and Medici (2006)	
CaO	52.69	52.27	49.81	50.18	51.09	50.33	51.70-54.30	48.69-51.98
Na_2O	1.56	1.67	3.36	3.07	2.58	3.09	0.13-2.26	2.53-3.88
P_2O_5	34.60	34.47	32.20	31.76	32.53	31.98	35.09-40.82	32.01-34.38
SO_3	7.42	8.33	11.54	11.71	11.79	12.58	0.40-7.39	8.21-11.40
F	3.32	2.64	2.81	2.64	1.49	1.32	3.26-3.33	0.00
Cl	0.41	0.61	0.27	0.63	0.52	0.69	0.00	1.19-1.91
Total	100.00	100.00	100.00	100.00	100.00	100.00		

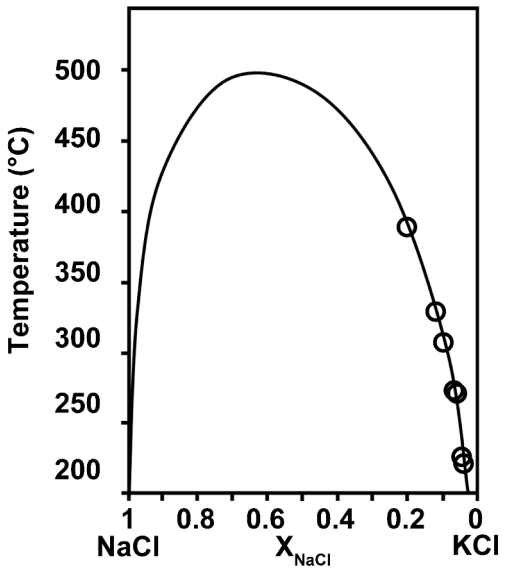

Figure 6. The two-phase region in the system NaCl-KCl, after Waldbaum (1969), reporting points which correspond to X_{NaCl} from microprobe analyses (Table 4).

sulphur fugacity can be induced by moderate fluctuation of oxidation state in the system, promoting the release of considerable amounts of sulphur from primary sulphides into the circulating aqueous fluids, or vice versa. In fact, petrological investigations on oceanic serpentinites evidenced that hydrothermal reaction of seawater with harzburgite at high temperatures (350-400 °C; Alt and Shanks III, 2003) during the early stage of serpentinization, dominated by low to moderate water/rock ratio and reducing conditions (Delacour et al., 2008), lead to the desulphurization of pentlandite into S-poor sulphides, i.e. heazlewoodite and magnetite (Klein and Bach, 2009), occasionally associated with godlevskite (Frost, 1985). S-rich sulphides (i.e., millerite and polydymite-ss) are usually generated in the late stage of serpentinization, as a consequence of their low solubility at temperature of about 300 °C.

The lack of magnetite and brucite, in the studied Hyblean peridotite xenoliths, is commonly attributed to hydration of olivine and pyroxene (see reaction 1), which leads to conditions unfavourable for their formation, governed by high a_{SiO_2} (between the Serpentine-Brucite and Serpentine-Talc buffers; Frost and Beard, 2007). The inferred silica enrichment in Hyblean serpentinized peridotites can be also explained by hydrothermal reaction of seawater with gabbros, according to experimental results and field observations in oceanic serpentinites from MAR (Mid-Atlantic Ridge) (Bach et al., 2004, and references therein), which report the formation in gabbros of albite, amphibole, chlorite, and Mg silicates (Bach and Klein, 2007). Similarly, Scribano et al. (2006b) investigated one of the numerous silicate metasomatite xenoliths in Hyblean tuff-breccia deposits, which bear evidence for alkaline and hydrous metasomatism, proven by a complex hydrothermal mineral assemblage including Na-rich alkali feldspar, mafic clays, Na-amphiboles, Fe-Ti oxides/hydroxides, sieved- textured aegirine-augite, titanite and zircons.

As the serpentinization reactions proceed to redox conditions above the PPM buffer (Pyrite-Pyrrhotite-Magnetite), S-rich sulphides become stable and the formation of millerite may occur at the expense of heazlewoodite or godlevskite (see reactions 3 and 4; Klein and Bach, 2009), which is successively replaced by polydymite (reaction 5):

(3) $Ni_3S_{2(s)} + H_2S_{(aq)} \rightarrow 3NiS_{(s)} + H_{2(aq)}$

(4) $Ni_9S_{8(s)} + H_2S_{(aq)} \rightarrow 9NiS_{(s)} + H_{2(aq)}$

(5) $3NiS_{(s)} + H_2S_{(aq)} \rightarrow Ni_3S_{4(s)} + H_{2(aq)}$

In association with the studied sulphide assemblage, some xenoliths bring evidence for incipient alteration of serpentine minerals by carbonate and poorly aluminous smectites (saponite; Figure 2G), particularly in sample P5 which contains diffuse grains of chalcedony.

This mineral assemblage can be referred to the low-temperature hydrothermal alteration of

serpentinized peridotites under conditions of high water/rock ratio (Bonatti et al., 1980) and high f_{O_2}, favoured by the circulation of hypersaline water solutions (Dufaud et al., 2009), which leads to hydrolysis of serpentine (see reaction 6) and pristine mafic minerals (Cipolli et al., 2004).

(6) $Mg_3Si_2O_5(OH)_4 + H_2O + (CO_3)^{2-}{}_{(aq)} + Ca^{2+}{}_{(aq)} \rightarrow CaCO_3 + 3Mg^{2+}{}_{(aq)} + 2SiO_2 + 6OH^-{}_{(aq)}$

The enrichment of Ca ions in hydrothermal solutions could derive from the transformation of seawater (Ca^{2+} = ~ 0.4 g/Kg; Bonatti et al., 1980) into hydrothermal solution (Amini et al., 2008; Eickmann et al., 2009), the dissolution of pyroxenes (Frost and Beard, 2007), as well as the albitization of plagioclase in gabbroic rocks belonging to Hyblean lower crust (Scribano et al., 2006b).

Moreover, the predominance of aragonite respect to calcite, as seen in serpentinite-hosted carbonate from modern and fossil spreading ridges, is confirmed by experimental results which demonstrated that Mg and Sr ions in hydrothermal fluids (Eickmann et al., 2009, and references therein) inhibit the formation of calcite.

Finally, the precipitation of chalcedony and clay minerals is possible (e.g., Cipolli et al., 2004) under the same conditions for carbonates. In particular, low-temperature submarine hydrothermal systems (20-150 °C; Aoki et al., 1996; Milliken et al., 1996) hosted in abyssal serpentinites are suitable environments for the formation of Fe-rich smectites, such as saponite, nontronite, montmorillonite.

Origin of (Ca, Na, S)-rich phosphate veinlets

Among the numerous phases constituting the secondary mineral assemblage inside serpentine veins, the occurrence of phosphate veinlets is noteworthy, which provides an evidence for reactions in an open system. Thus, a magmatic origin of this mineral, in the eruptive system bearing the xenoliths, would be supported by high P_2O_5 content (Suiting and Schmincke, 2009) in the juvenile nephelinite clasts.

However, the hydrothermal origin of phosphate veinlets can be inferred on the basis of (1) direct precipitation of (Na, S)-rich fluorapatites from F-rich hydrothermal solutions at 200-250 °C (Shiga and Urashima, 1987), in agreement with the hydrothermal synthesis of phosphate-sulphate fluorapatites (Piotrowski et al., 2004), and (2) the SO_3 amounts which vary from 0.04 to 0.63 wt% (Peng et al., 1997) in apatite crystals found in volcanic rocks, unlike hydrothermal apatites which can contain more than 7 wt% of sulphate ions (Shiga and Urashima, 1987).

Moreover, the occurrence of hydrothermal phosphate veinlets could be considered a possible source of LREE (light rare earth elements) enrichment in Hyblean peridotites, although it was previously attributed to a cryptic metasomatic event (Perinelli et al., 2008; Tonarini et al., 1996). In particular, Tonarini et al. (1996) demonstrated that the enrichment of LREE and other incompatible elements cannot be attributed to contamination by host lavas, but to a metasomatic event dated back to Permo-Triassic age, which correspond with timing of the fossil hydrothermal system inferred by Scribano et al. (2006b). The latter Authors asserted that the LREE and alkali enrichments in mafic Hyblean xenoliths are the result of chemical and mineralogical transformations, e.g. albitization of plagioclase, induced by hydrothermal fluids. In the same way, Sansoni et al. (2011) investigated some mafic rocks associated with serpentinized peridotites from Ligurian ophiolites (southern Appenines, Italy), in which they recognized mineral assemblages typical of oceanic crust in MAR, even including apatites and zircons as accessory phases. The same Authors remarked that the analysed rocks have chondrite-normalized REE patterns exhibiting LREE enrichment [$(La/Sm)_N > 1$], but negligible Eu anomaly, which they certainly

attributed to hydrothermal alteration.

In this regard, it is noteworthy to report that apatite-bearing serpentinites,found in an oceanic core-complex in Mid-Atlantic Ridge (Boschi et al., 2006, and references therein; Cannat et al., 1992), contain an average amount of P_2O_5 of 0.04 ± 0.02 wt%, in addition to La (0.17 ± 0.12 ppm) and Ce (0.47 ± 0.37 ppm). Hydrothermal apatite crystals occurring in Othrys ophiolite complex, central Greece (Mitsis and Economou-Eliopoulos, 2001), are characterized by a considerable LREE enrichment (La = 312-569 ppm, Ce = 365-686 ppm).

These evidence are supported by experimental results of seawater-driven serpentinization on harzburgites (Menzies et al., 1993), which confirmed that the enrichment in LREE can be attributed only to Ca-bearing secondary minerals (e.g., carbonates), rather than clinopyroxenes, due to the similarity of their ionic radii to that of Ca ion in octahedral coordination (Allen and Seyfried, 2005). Furthermore, chondrite-normalized REE patterns of fluids released from serpentinite-hosted hydrothermal systems in MAR, exhibit enrichment in LREE and other metals occurring in trace amounts (i.e. Mn, Fe, Co, Ni, Cu, Zn, Ag, Cd, Cs, Pb, Y, Zr, Th), whose complexation is enhanced by ligands such as Cl^-, F^-, OH^-, CO_3^{2-}, PO_4^{2-}, SO_4^{2-} (Mayanovic et al., 2009). Accordingly, the LREE enrichment in MARK serpentinites was attributed to seawater-driven serpentinization (Alt and Shanks III, 2003), although it was previously referred to a cryptic metasomatic event (Stephens, 1997).

Whole-rock geochemical data on the studied serpentinized harzburgite xenoliths (Table 1; Punturo, 1999) show an average concentration of P_2O_5 of 0.14 ± 0.04 wt%, in addition to La (1.15 ± 0.68 ppm) and Ce (0.822 ppm, up to 8.12 ppm in sample P5), similar to the above cited values in oceanic serpentinites. Nevertheless, the correlation between LREE enrichment and the presence of phosphate veinlets cannot be certainly demonstrated beyond doubt, because their extreme narrowness and thinness made it difficult to perform any quantitative microanalyses of trace elements.

Timing of serpentinization

A crucial question is to ascertain whether serpentinization affecting Hyblean peridotites could be referred to their pre- or post-eruptive stage, since all Hyblean xenoliths bear evidences for a variable degree of alteration produced by interaction with the host magma during its rising up till to the final diatremic eruption, and the post-depositional stage (Scribano et al., 2009).

The hypothesis of a post-depositional alteration is likely, because diatreme eruption at Valle Guffari occurred in a shallow marine environment, which was followed by low-temperature alteration of primary minerals forming the tuff-breccia deposit, Tortonian in age (Carlentini Fm.; Carbone and Lentini, 1981). The latter is constituted of lapilli-sized clasts of Ne-normative basanitoid juvenile lava with OIB affinity, predominantly glassy, and inequigranular lithics cemented by calcite and zeolites (Punturo and Scribano, 1997). If this hypothesis was true, serpentinization of peridotite xenoliths would be represented by the formation of a mineral assemblage compatible with low temperature hydration of pristine minerals, under oxidizing conditions above the Hematite-Magnetite buffer (Frost, 1985), which would induce the oxidization of primary sulphide minerals to pyrite and hematite (Alt and Shanks III, 2003).

On the contrary, mineralogical investigations on the studied partially serpentinized xenoliths, evidenced the occurrence of abundant secondary S-poor sulphides (i.e., godlevskite and heazlewoodite), as well as NaCl-KCl solid-solutions. This secondary mineral assemblage is certainly incompatible with the first hypothesis because (1) the identified sulphide minerals are stable under conditions of f_{O_2} ranging from -32 to -40 (Frost, 1985), and (2) salt solid-solutions form only at temperature higher than 200 °C

(Waldbaum, 1969). The possibility that clues to serpentinization would be erased by a high-temperature alteration, owing to interaction with magma, can be even excluded. In fact, Sapienza and Scribano (2000, and references therein) asserted that deep-seated xenoliths hosted in diatremic tuff-breccia deposits were preserved by similar reaction, as a consequence of the relatively low eruptive temperatures and the high ascending velocity of the eruptive column. Accordingly, Scribano et al. (2007) supposed that diatreme eruption, in Hyblean area, could be the result of interaction of the uprising basaltic magma with the deeper level of hydrothermally-modified Hyblean lower crust. The result would be the rapid dehydration of serpentinites, which generally contain an estimated quantity of water of about 250-400 $Kg \cdot m^3$ (Carlson, 2001), followed by brecciation of country rocks and fluidization of the system. This hypothesis is supported by evidence of hydrofracture in oceanic lithosphere, induced by fluid overpressure due to antigorite dehydration reaction (Miller et al., 2003, and references therein).

For these reasons, a likely hypothesis could be that serpentinization came before the eruptive stage, Tortonian in age (Carbone and Lentini, 1981). But, a more precise constraint on the timing of early serpentinization, in Hyblean lithospheric basement, derives from hydrothermal zircons, hosted in a blackwall-type metasomatie xenolith (Scribano et al., 2006b), according to Dubińska et al. (2004). Hyblean hydrothermal zircons were dated back to Early Triassic by in situ U-Pb analyses (~ 246 My; Sapienza et al., 2007).

Conclusions

This paper reports mineralogical investigations on seven Hyblean harzburgite xenoliths, which bear evidence for serpentinization represented by serpentine veins and their related secondary minerals. Analytical results demonstrated that two serpentine polytypes occur in composite veins, i.e. chrysotile $2M_{c1}$ and lizardite $1T$, which probably formed in the temperature range of ~ 250 °C up to 350-400 °C (Bach et al., 2004, and references therein), at pressure below 0.2 GPa (Mével, 2003) as confirmed by the lack of antigorite polymorphs, whose stability field ranges from prehnite-pumpellyite facies to amphibolite facies (Mellini et al., 1987).

The composition of altering fluids can be inferred by the presence of chloride both as ions and interstitial grains in serpentine, which suggests that serpentinization process was triggered by seawater-peridotite interaction, as commonly observed in oceanic serpentinized peridotites (e.g., Miura et al., 1981; Scambelluri et al., 1997; Sharp and Barnes, 2004).

Additionally, serpentine veins contain other secondary minerals, which are sulphides, aragonite and saponite, that provide constraints on physico-chemical conditions during serpentinization. Most of the studied xenoliths enclose S-poor sulphides ($S/M < 1$), such as heazlewoodite and godlevskite, which represent a mineral assemblage typical of incipient serpentinization (Klein and Bach, 2009), characterized by reducing conditions (above the Iron-Magnetite buffer) at high temperature (~ 400 °C; Fleet, 1988), and low to moderate water/rock (W/R) ratio. Two samples, instead, contain a second mineral assemblage constituted of S-rich sulphides ($S/M > 1$), i.e. millerite and polydymite-ss, in addition to saponite and aragonite, which are indicative of relatively oxidizing conditions (f_{O_2} from -32 to -30), low temperature (~ 280-100 °C; Fleet, 1988; Aoki et al., 1996; Milliken et al., 1996), and high W/R ratio.The occurrence of these two assemblages, hosted in serpentine veins, would suggest that secondary minerals formed during two different stages of serpentinization (Figure 7), as commonly observed in oceanic serpentinites (e.g., Bach et al., 2004; Alt and Shanks III, 2003; Frost, 1985). In this regard, the considered

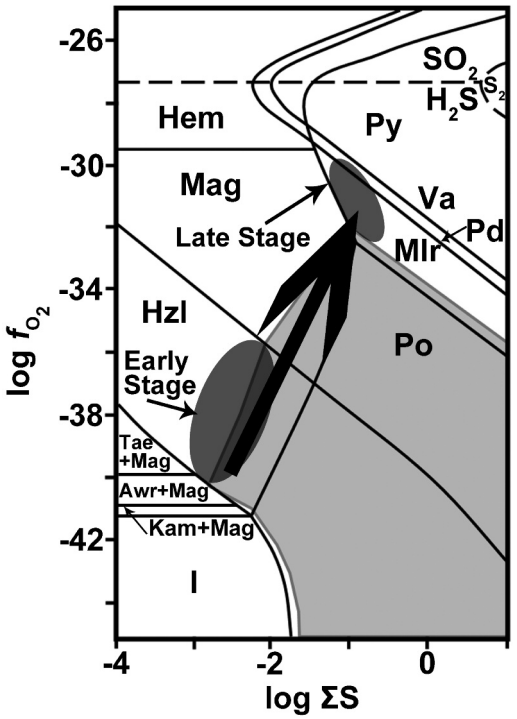

Figure 7. Log ΣS vs log fo_2 (where ΣS is the sum of the activities of the sulphur species) diagram showing the stability fields of oxides and sulphides during serpentinization process (simplified after Frost, 1985). Heavy solid lines are mineral reaction boundaries at 300 °C and 2 kbar, and dashed lines mark boundaries between dominant sulphur species. The shaded area represents the stability field of pentlandite. The black arrow indicates the evolution of serpentinization reactions in the ultramafic rocks of the Hyblean Plateau, which proceeds from the early stage (heazlewoodite + godlevskite) gradually to the late stage (millerite + polydymite). Mineral abbreviations: Awr: awaruite; Hem: hematite; Hzl: heazlewoodite; I: iron; Kam: kamacite; Mlr: millerite; Mag: magnetite; Pd: polydymite; Po: pyrrhotite; Py: pyrite; Tae: taenite; Va: vaesite.

xenoliths could derive from two portions of Hyblean ultramafic core-complex (Scribano et al., 2006a), in which serpentinization proceeded in the same time, but under contrasting environmental conditions (*T*, *W/R* ratio, f_{O_2}) at different depths. Alternatively, the same samples could represent two different period of serpentinization, probably due to the uplift of Hyblean lower crust. In fact, Scribano and Manuella (2008) inferred that Hyblean basement underwent important volume increase by serpentinization of peridotites during non-magmatic periods, as evidenced by disequilibrium textures found in some Hyblean xenoliths (websterites and metagabbros). This evidence is in accordance with experimental and field observations (Iyer et al., 2008), which demonstrated the capacity of serpentinized ultramafic rocks to produce an uplift of 10^2 - 10^3 m at a rate of mm·y^{-1} to cm·y^{-1} (Skelton and Jakobsson, 2007).

Both hypotheses are likely, and neither can be excluded on the basis of reported petrological and mineralogical data, which need to be improved by further studies of Hyblean serpentinized xenoliths. Nevertheless, the same results seem to be in agreement with the geological model proposed by Scribano et al. (2006a, b), of an ultramafic core-complex forming the Hyblean lower crust, which was altered by a long-lasting hydrothermal circulation of seawater penetrated through deep fracture systems.

Acknowledgements

This paper is part of the Ph.D. thesis of F.C.M., financially supported by the Università di Catania (grants for Ph.D. researches). I am grateful to proff. M. Lustrino and A. Gianfagna for their editorial assistance, as well as to Drs. C. Perinelli and S. Tumiati, for their careful review and constructive comments to the manuscript. Moreover, I wish to thank prof. R.R. Carrabino, for her accurate revision of English language, and prof. V. Scribano, who provided the seven thin sections of harzburgite xenoliths.

References

Allen D. and Seyfried W.E. Jr. (2005) - REE controls in ultramafic hosted MOR hydrothermal systems: An experimental study at elevated temperature and pressure. *Geochimica et Cosmochimica Acta*, 69, 675-683.

Alt J.C. and Shanks III W.C. (2003) - Serpentinization of abyssal peridotites from the MARK area, Mid-Atlantic Ridge: sulfur geochemistry and reaction modelling. *Geochimica et Cosmochimica Acta*, 67, 641-653.

Amini M., Eisenhauer A., Böhm F., Fietzke J., Bach W., Garbe-Schönberg D., Rosner M., Bock B., Lackschewitz K.S. and Hauff F. (2008) - Calcium isotope ($\delta^{44/40}$Ca) fractionation along hydrothermal pathways, Logatchev field (Mid-Atlantic Ridge, 14°45′N). *Geochimica et Cosmochimica Acta*, 72, 4107-4122.

Andreani M., Baronnet A., Boullier A.M. and Gratier J.P. (2004) - A microstructural study of a crack-seal type serpentine vein, using SEM and TEM techniques. *European Journal of Mineralogy*, 16, 585-595.

Anselmi B., Mellini M. and Viti C. (2000) - Chlorine in the Elba, Monti Livornesi and Murlo serpentines: evidence for sea-water interaction. *European Journal of Mineralogy*, 12, 137-146.

Aoki S., Kohyama N. and Hotta H. (1996) - Hydrothermal clay minerals found in sediment containing yellowish-brown material from the Japan Basin. *Marine Geology*, 129, 331-336.

Bach W. and Früh-Green G.L. (2010) - Alteration of the oceanic lithosphere and implications for seafloor processes. *Elements*, 6, 173-178.

Bach W. and Klein F. (2007) - Silica metasomatism of oceanic serpentinites. *Geochimica et Cosmochimica Acta*, 71, A48.

Bach W., Garrido C.J., Paulick H., Harvey J. and Rosner M. (2004) - Seawater-peridotite interactions: First insights from ODP Leg 209, MAR 15 N. *Geochemistry Geophysics Geosystems*, 5, 1-22.

Beccaluva L., Di Grande A., Lo Giudice A. and Siena F. (1991) - Geopetrographic map of Northern-central Iblean area (South-eastern Sicily). Scale 1:50000.

Bianchini G., Bell K. and Vaccaro C. (1999) - Mantle sources of the Cenozoic Iblean volcanism (SE Sicily, Italy): Sr-Nd-Pb isotopic constraints. *Mineralogy and Petrology*, 67, 213-222.

Bonatti E., Lawrence J.R., Hamlyn P.R. and Breger D. (1980) - Aragonite from deep sea ultramafic rocks. *Geochimica et Cosmochimica Acta*, 44, 1207-1214.

Boschi C., Früh-Green G.L., Delacour A., Karson J.A. and Kelley D.S. (2006) - Mass transfer and fluid flow during detachment faulting and development of an oceanic core complex, Atlantis Massif (MAR 30°N). *Geochemistry Geophysics Geosystems*, 7, Q01004.

Brancato A., Hole J.A., Gresta S. and Beale J.N. (2009) - Determination of seismogenic structures in Southeastern Sicily (Italy) by high-precision relative relocation of microearthquakes. *Bulletin of Seismological Society of America*, 99, 1921-1936.

Cannat M., Bideau D. and Bougault H. (1992) - Serpentinized peridotites and gabbros in the Mid-Atlantic Ridge axial valley at 15°37'N and 16°52'N. *Earth and Planetary Science Letters*, 109, 87-106.

Carlson R.L. (2001) - The abundance of ultramafic rocks in Atlantic Ocean crust. *Geophysical Journal International*, 144, 37-48.

Catalano R., Franchino A., Merlini S. and Sulli A. (2000) - A crustal section fromthe Eastern Algerian basin to the Ionian ocean (Central Mediterranean). *Memorie della Società Geologica Italiana*, 55, 71-86.

Chakhmouradian A.R. and Medici L. (2006) - Clinohydroxylapatite: a new apatite-group mineral from northwestern Ontario (Canada), and new data on the extent of Na-S substitution in natural apatites. *European Journal of Mineralogy*, 18, 105-112.

Ciliberto E., Crisafulli C., Manuella F.C., Samperi F., Scirè S., Scribano V., Viccaro M. and Viscuso E. (2009) - Aliphatic hydrocarbons in metasomatized gabbroic xenoliths from Hyblean diatremes (Sicily): Genesis in a serpentinite hydrothermal system. *Chemical Geology*, 258, 258-268.

Cipolli F., Gambardella B., Marini L., Ottonello G. and Vetuschi Zuccolini M. (2004) - Geochemistry of high-pH waters from serpentinites of the Gruppo di Voltri (Genova, Italy) and reaction path modelling of CO_2 sequestration in serpentinite aquifers. *Applied Geochemistry*, 19, 787-802.

Delacour A., Früh-Green G.L. and Bernasconi S.M. (2008) - Sulfur mineralogy and geochemistry of

serpentinites and gabbros of the Atlantis Massif (IODP Site U1309). *Geochimica et Cosmochimica Acta*, 72, 5111-5127.

Dias A.S. and Barriga F.J.A.S. (2006) - Mineralogy and geochemistry of hydrothermal sediments from the serpentinite-hosted Saldanha hydrothermal field (36°34′N; 33°26′W) at MAR. *Marine Geology*, 225, 157-175.

Dubińska E., Bylina P., Kozłowski A., Dörr W., Nejbert K., Scastock J. and Kulicki C. (2004) - U-Pb dating of serpentinization: hydrothermal zircon from metosomatic rodingite shell (Sudetic Ophiolite, SW Poland). *Chemical Geology*, 203, 183-203.

Dufaud F., Martinez I. and Shilobreeva S. (2009) - Experimental study of Mg-rich silicates carbonation at 400 and 500 °C and 1 kbar. *Chemical Geology*, 262, 344-352.

Eickmann B., Bach W. and Peckmann J. (2009) - Authigenesis of carbonate minerals in modern and Devonian ocean-floor hard rocks. *Journal of Geology*, 117, 307-323.

Emmanuel S. and Berkowitz B. (2006) - Suppression and stimulation of seafloor hydrothermal convection by exothermic mineral hydration. *Earth and Planetary Science Letters*, 243, 657-668.

Fleet M.E. (1988) - Stoichiometry, structure and twinning of godlevskite and synthetic low-temperature Ni-excess nickel sulfide. *Canadian Mineralogist*, 26, 283-291.

Frost R.B. (1985) - On the stability of sulphides, oxides, and native metals in serpentinite. *Journal of Petrology*, 26, 31-63.

Frost R.B. and Beard J.S. (2007) - On silica activity and serpentinization. *Petrology*, 48, 1351-1368.

Horen H., Zamora M. and Dubuisson G. (1996) - Seismic waves velocities and anisotropy in serpentinized peridotites from Xigaze ophiolite: Abundance of serpentine in slow spreading ridge. *Geophysics Research Letters*, 23, 9-12.

Hostetler P.B., Coleman R.G., Mumpton F.A. and Evans B.W. (1966) - Brucite in Alpine serpentinites. *American Mineralogist*, 5l, 75-98.

Iyer K., Austrheim H., John T. and Jamtveit B. (2008) - Serpentinization of the oceanic lithosphere and some geochemical consequences: Constraints from the Leka Ophiolite Complex, Norway. *Chemical Geology*, 249, 66-90.

Klein F. and Bach W. (2009) - Fe-Ni-Co-O-S phase relations in peridotite-seawater interactions. *Journal of Petrology*, 50, 37-59.

Korytkova E.N., Pivovarova L.N. and Gusarov V.V. (2007) - Influence of iron on the kinetics of formation of chrysotile nanotubes of composition $(Mg, Fe)_3Si_2O_5(OH)_4$ under hydrothermal conditions. *Geochemistry International*, 45, 825-831.

Koschinsky A., Garbe-Schönberg D., Sander S., Schmidt K., Gennerich H.-H. and Strauss H. (2008) - Hydrothermal venting at pressure-temperature conditions above the critical point of seawater, 5°S on the Mid-Atlantic Ridge. *Geology*, 36, 615-618.

Le Mée L., Girardeau J. and Monnier C. (2004) - Mantle segmentation along the Oman ophiolite fossil mid-ocean ridge. *Nature*, 432, 167-172.

Lentini F., Carbone S., Catalano S. and Grasso M. (1996) - Elementi per la ricostruzione del quadro strutturale della Sicilia orientale. *Memorie della Società Geologica Italiana*, 51, 179-195.

MacDonald A.H. and Fyfe W.S. (1985) - Rate of serpentinization in seafloor environments. *Tectonophysics*, 116, 123-135.

Mayanovic R.A., Anderson A.J., Bassett W.A. and Chou I.M. (2009) - Steric hindrance and the enhanced stability of light rare-earth elements in hydrothermal fluids. *American Mineralogist*, 94, 1487-1490.

Mellini M., Trommsdorff V. and Compagnoni R. (1987) - Antigorite polysomatism: behaviour during progressive metamorphism. *Contribute to Mineralogy and Petrology*, 97, 147-155.

Menzies M.A., Long A., Ingram G., Tatnell M.V. and Janecky D. (1993) - MORB peridotite-sea water interaction: experimental constraints on the behaviour of trace elements, $^{87}Sr/^{86}Sr$ and $^{143}Nd/^{144}Nd$ ratios. *Geological Society Special Publication*, 76, 309-322.

Mével C. (2003) - Serpentinization of abyssal peridotites at mid-ocean ridges. *Geomaterials*, 335, 825-852.

Miller S.A., van der Zee W., Olgaard D.L. and Connolly J.A.D. (2003) - A fluid-pressure feedback model of dehydration reactions: experiments, modelling, and application to subduction zones. *Tectonophysics*, 370, 241-251.

Milliken K.L., Lynch F.L. and Seifert K.E. (2004) - Marine weathering of serpentinites and serpentinite breccias, Sites 897 and 899, Iberia abyssal plain.

Proceedings of the Ocean Drilling Project Scientific Results, 149, 529-540.

Misra K.C. and Fleet M.E. (1974) - Chemical composition and stability of violarite. *Economic Geology,* 69, 391-403.

Mitsis I. and Economou-Eliopoulos M. (2001) - Occurrence of apatite associated with magnetite in an ophiolite complex (Othrys), Greece. *American Mineralogist*, 86, 1143-1150.

Miura Y., Rucklidge J. and Nord G.L. Jr. (1981) - The occurrence of chlorine in serpentine minerals. *Contributions to Mineralogy and Petrology*, 76, 17-23.

Oufi O. and Cannat M. (2002) - Magnetic properties of variably serpentinized abyssal peridotites. *Journal of Geophysical Research*, 107.

Parthasarathy G., Choudary B.M., Sreedhar B., Kunwar A.C. and Srinivasan R. (2003) - Ferrous saponite from the Deccan Trap, India, and its application in adsorption and reduction of hexavalent chromium. *American Mineralogist*, 88, 1983-1988.

Peng G., Luhr J.F. and McGee J.J. (1997) - Factors controlling sulfur concentrations in volcanic apatite. *American Mineralogist*, 82, 1210-1224.

Perinelli C., Sapienza G.T., Armienti P. and Morten L. (2008) - Metasomatism of the upper mantle beneath the Hyblean Plateau (Sicily): evidence from pyroxenes and glass in peridotite xenoliths. *Geological Society Special Publication*, 293, 197-221.

Pikovskii Y.I., Chernova T.G., Alekseeva T.A. and Verkhovskaya Z.I. (2004) - Composition and nature of hydrocarbons in modern serpentinization areas in the ocean. *Geochemistry International*, 42, 971-976.

Piotrowski A., Kahlenberg V. and Fischer R. (2004) - Mixed phosphate-sulfate fluorapatites as possible materials in dental fillers. *European Journal of Mineralogy*, 16, 279-284.

Punturo R. (1999) - Caratterizzazione petrologica e petrofisica di xenoliti di origine profonda nelle tufo-brecce mioceniche della Valle Guffari (Altopiano Ibleo, Sicilia). Ph.D. dissertation, Università di Catania, 138 pp.

Punturo R. and Scribano V. (1997) - Dati geochimici e petrografici su xenoliti di clinopirossenite a grana ultragrossa e websteriti nelle vulcanoclastiti mioceniche dell'Alta Valle Guffari (Monti Iblei, Sicilia). *Mineralogica et Petrografica Acta*, 40, 95-116.

Punturo R., Kern H., Scribano V. and Atzori P. (2000) - Petrophysical and petrological characteristics of deep-seated xenoliths from the Hyblean Plateau, south-eastern Sicily, Italy: suggestions for a lithospheric model. *Mineralogica et Petrografica Acta*, 43, 1-20.

Ribeiro da Costa I., Barriga F.J.A.S. and Taylor R.N. (2008) - Late seafloor carbonate precipitation in serpentinites from Rainbow and Saldanha sites (Mid-Atlantic Ridge). *European Journal of Mineralogy*, 20, 173-181.

Riordon P.H. (1955) - The genesis of asbestos in ultrabasic rocks. *Economic Geology*, 50, 67-81.

Saito Y., Goldbeck-Wood G. and Müller-Krumbhaar H. (1987) - Dendritic pattern formation. *Physica Scripta*, T19, 327-329.

Sansone M.T.C., Rizzo G. and Mongelli G. (2011) - Petrochemical characterization of mafic rocks from the Ligurian ophiolites, southern Apennines. *International Geology Review*, 53, 130-156.

Sapienza G. and Scribano V. (2000) - Distribution and representative whole-rock chemistry of deep-seated xenoliths from the Iblean Plateau, south-eastern Sicily, Italy. *Periodico di Mineralogia*, 69, 185-204.

Sapienza G., Griffin W.L., O'Reilly S.Y. and Morten L. (2007) - Crustal zircons and mantle sulfides: Archean to Triassic events in the lithosphere beneath south-eastern Sicily. *Lithos*, 96, 503-523.

Scambelluri M., Piccardo G.B., Philippot P., Robbiano A. and Negretti L. (1997) - High salinity fluid inclusions formed from recycled seawater in deeply subducted alpine serpentinite. *Earth and Planetary Science Letters*, 148, 485-499.

Schmidt K., Koschinsky A., Garbe-Schönberg D., de Carvalho L.M. and Seifert R. (2007) - Geochemistry of hydrothermal fluids from the ultramafic-hosted Logatchev hydrothermal field, 15°N on the Mid-Atlantic Ridge: Temporal and spatial investigation. *Chemical Geology*, 242, 1-21.

Schroeder T., John B. and Frost B.R. (2002) - Geologic implications of seawater circulation through peridotite exposed at slow-spreading mid-ocean ridges. *Geology*, 30, 367-370.

Scribano V. (1986) - The harzburgite xenoliths in a Quaternary basanitoid lava near Scordia (Hyblean plateau, Sicily). *Rendiconti SIMP*, 41, 245-255.

Scribano V. (1987) - The ultramafic and mafic nodule

suite in a tuff-breccia pipe from Cozzo Molino (Hyblean Plateau, SE Sicily). *Rendiconti SIMP*, 42, 203-217.

Scribano V. and Manuella F.C. (2008) - Early seafloor exposure of Hyblean uppermost mantle and prime role of serpentinization for plateau uplifting: a xenolith perspective. Atti del Congresso "Tethys to Mediterranean: a journey of geological discovery", Catania 3rd-5th June 2008, 103.

Scribano V., Carbone S. and Manuella F.C. (2007) - Diatreme eruption probably related to explosive interaction of rising magma with serpentinite diapirs in the shallow crust (Carlentini Formation, Hyblean area, Sicily): a xenolith perspective. *Epitome*, 2, 130-131.

Scribano V., Ioppolo S. and Censi P. (2006b) - Chlorite/smectite-alkali feldspar metasomatica xenoliths from Hyblean Miocenic diatremes (Sicily, Italy): evidence for early interaction between hydrothermal brines and ultramafic/mafic rocks at crustal levels. *Ofioliti*, 31, 161-171.

Scribano V., Sapienza G.T., Braga R. and Morten L. (2006a) - Gabbroic xenoliths in tuffbreccia pipes from the Hyblean Plateau: insights into the nature and composition of the lower crust underneath South-Eastern Sicily, Italy. *Mineralogy and Petrology*, 86, 63-88.

Scribano V., Viccaro M., Cristofolini R. and Ottolini L. (2009) - Metasomatic events recorded in ultramafic xenoliths from the Hyblean area (Southeastern Sicily, Italy). *Mineralogy and Petrology*, 95, 235-250.

Sharp Z.D. and Barnes J.D. (2004) - Water-soluble chlorides in massive seafloor serpentinites: a source of chloride in subduction zones. *Earth and Planetary Science Letters*, 226, 243-254.

Shiga Y. and Urashima Y. (1987) - A sodian sulfatian fluorapatite from an epithermal calcite-quartz vein of the Kushikino Mine, Kagoshima Prefecture, Japan. *Canadian Mineralogist*, 25, 673-681.

Silantyev S.A., Mironenko M.V. and Novoselov A.A. (2009) - Hydrothermal systems in peridotites of slow-spreading mid-oceanic ridges. Modeling phase transitions and material balance: downwelling limb of a hydrothermal circulation cell. *Petrology*, 17, 138-157.

Skelton A. and Jakobsson M. (2007) - Could peridotite hydration reactions have provided a contributory driving force for Cenozoic uplift and accelerated subsidence along the margins of the North Atlantic and Labrador Sea? *Norwegian Journal of Geology*, 87, 21-28,

Southgate P.N. (1982) - Cambrian skeletal halite crystals and experimental analogues. *Sedimentology*, 29, 391-407.

Stephens C.J. (1997) - Heterogeneity of oceanic peridotite from the western canyon wall at MARK: Results from site 920. *Proceedings of the Ocean Drilling Project Scientific Results*, 153, 285-304.

Suiting I. and Schmincke H.U. (2009) - Internal vs. external forcing in shallow marine diatreme formation: A case study from the Iblean Mountains (SE-Sicily, Central Mediterranean). *Journal of Volcanology and Geothermal Research*, 186, 361-378.

Tonarini S., D'Orazio M., Armenti P., Innocenti F. and Scribano V. (1996) - Geochemical features of Eastern Sicily lithosphere as probed by Hyblean xenoliths and lavas. *European Journal of Mineralogy*, 8, 1153-1173.

Trommsdorff V., Skippen G. and Ulmer P. (1985) - Halite and sylvite as solid inclusions in high-grade metamorphic rocks. *Contributions to Mineralogy and Petrology*, 89, 24-29.

Trua T., Esperança S. and Mazzuoli R. (1998) - The evolution of the lithospheric mantle along the N. African Plate: geochemical and isotopical evidence from the tholeiitic and alkaline volcanic rocks of the Hyblean plateau, Italy. *Contributions to Mineralogy and Petrology*, 131, 307-322.

Ueno T., Ito S.-i. and Nakatsuka S. (2000) - Phase equilibria in the system Fe-Ni-S at 500 °C and 400 °C. *Journal of Mineralogical and Petrological Sciences*, 95, 145-161.

Vai G.B. (2003) - Development of the palaeogeography of Pangea from Late Carboniferous to Early Permian. *Palaeo*, 196, 125-155.

Viti C. and Mellini M. (1997) - Contrasting chemical compositions in associated lizardite and chrysotile in veins from Elba, Italy. *European Journal of Mineralogy*, 9, 585-596.

Waldbaum D.R. (1969) - Thermodynamic mixing properties of NaCl-KCl liquids. *Geochimica et Cosmochimica Acta*, 33, 1415-1427.

Submitted, September 2010 - Accepted, April 2011